Inorganic Chemistry
Article

Inorg. Chem. **2009**, *48*, 6391–6401 **6391**
DOI: 10.1021/ic900629t

Theoretical Interpretation of the Structural Variations along the $Eu(Zn_{1-x}Ge_x)_2$ ($0 \leq x \leq 1$) Series

Tae-Soo You and Gordon J. Miller*

Department of Chemistry, Iowa State University, Ames, Iowa 50011

Received March 31, 2009

The electronic structures of $EuZn_2$, $Eu(Zn_{0.75}Ge_{0.25})_2$, $Eu(Zn_{0.5}Ge_{0.5})_2$, $Eu(Zn_{0.25}Ge_{0.75})_2$, and $EuGe_2$ have been investigated using tight-binding, linear muffin-tin orbital (TB-LMTO) and pseudopotential methods to understand the structural preferences influenced by valence electron counts and to explain the observed homogeneity range of the AlB_2-type phases as reported in the companion article. A crystal orbital Hamilton population (COHP) analysis for Zn−Zn contacts in $EuZn_2$ suggests a possible homogeneity width for the KHg_2-type phase, which is indicated from analysis of X-ray powder diffraction patterns. Total electronic energy comparisons, as well as density of states (DOS) and COHP analysis for a hypothetical Zn-rich compound, $Eu(Zn_{0.75}Ge_{0.25})_2$, indicate that two distinct phases, KHg_2-type $EuZn_2$ and AlB_2-type $Eu(Zn_{1-x}Ge_x)_2$ ($0.5 \leq x \leq 0.70$), are more favorable than a single Zn-rich composition adopting the AlB_2-type phase. Among 10 structural models of $Eu(Zn_{0.5}Ge_{0.5})_2$, the one with heteroatomic Zn−Ge interactions both within and perpendicular to the 6^3 nets is energetically the most favorable structure. The experimentally observed Zn−Ge bond distance is attributed to the contribution of both σ- and π-bond interactions. Zn−Ge, Eu−Zn, and Eu−Ge COHP curves of the minimum energy form of $Eu(Zn_{0.5}Ge_{0.5})_2$ show bonding character above the Fermi level and explain the observed wide homogeneity width of the AlB_2-type phase. In the Ge-rich case, $Eu(Zn_{0.25}Ge_{0.75})_2$, the planar hexagonal nets are not energetically favorable due to the significant antibonding character of Ge−Ge bonding at the Fermi level. Structural relaxation using pseudopotentials also revealed that the hexagonal nets tend to pucker rather than being planar, in agreement with the observed incommensurately modulated superstructure. An electron localization function analysis for $Eu(Zn_{0.5}Ge_{0.5})_2$ reveals that there exists no two-center, two-electron bond or multicentered interactions between interlayer Zn···Ge contacts.

Introduction

During our systematic investigations of the $Eu(M_{1-x}M'_x)_2$ series (M, M′ = group 12−14 elements) to study the interrelationships among atomic, electronic, and possible magnetic structures by varying atomic sizes and valence electron counts, we have observed a systematic structural variation within the $Eu(Zn_{1-x}Ge_x)_2$ system as x increases from the KHg_2-type to the AlB_2-type and, finally, the $EuGe_2$-type structure.[1] These structure types differ in the networks formed by the electronegative Zn/Ge components: (a) the KHg_2 type adopts a four-bonded, three-dimensional (4b-3D) net with locally distorted tetrahedral coordination; (b) the AlB_2 type contains three-bonded, two-dimensional (3b-2D) planes with trigonal-planar coordination; and (c) the $EuGe_2$ type exhibits 3b-2D puckered nets with local trigonal-pyramidal environments. Furthermore, an incommensurately modulated stacking along the c direction was observed for the nine-electron case, $Eu(Zn_{0.25}Ge_{0.75(2)})_2$. Application of the Zintl−Klemm formalism[2−4] to these $Eu(Zn_{1-x}Ge_x)_2$ phases showed limited validity: $x = 0.50(2)$, that is, EuZnGe, represents the lower limit of the AlB_2-type phases, which contains formally "Ge^{4-}" sites with no short Ge−Ge contacts. The upper bound for this region, that is, $x = 0.75(2)$, however, could not be rationalized by this simple electron counting approach.[1]

The transition from planar to puckered three-connected polyanionic nets is clearly related to the number of valence s and p electrons at the electronegative components,[5,6] while the occurrence of 4b-3D tetrahedral versus 3b-2D planar nets relies on an interplay of both electronegativity and size effects.[7] In a recent study of EuGaTt (Tt = Si, Ge, Sn),[8] atomic size also influences puckering of 3b-2D nets, which is further mediated by the role of valence s and d orbitals at the active metal site, that is, Eu, by creating multicenter

*To whom correspondence should be addressed. E-mail: gmiller@iastate.edu.

(1) You, T.-S; Lidin, S.; Gourdon, O.; Wu, Y.; Miller, G. J. *Inorg. Chem.* **2009**, companion article.

(2) Nesper, R. *Prog. Solid State Chem.* **1990**, *20*, 1.
(3) Miller, G. J. In *Chemistry, Structure, and Bonding of Zintl Phases and Ions*; Kauzlarich, S. M., Ed.; VCH Publishers: New York, 1996; p 1.
(4) Schäfer, H. *Annu. Rev. Mater. Sci.* **1985**, *5*, 1.
(5) Zheng, C.; Hoffmann, R. *Inorg. Chem.* **1989**, *28*, 1074.
(6) Hoffman, R.-D.; Pöttgen, R. *Z. Kristallogr.* **2001**, *216*, 127.
(7) Burdett, J. K.; Miller, G. J. *Chem. Mater.* **1990**, *2*, 12.
(8) You, T.-S.; Grin, Y.; Miller, G. J. *Inorg. Chem.* **2007**, *46*, 8801.

© 2009 American Chemical Society
Published on Web 06/16/2009

interactions. In this work, we explore the electronic structures of the $Eu(Zn_{1-x}Ge_x)_2$ ($0 \le x \le 1$) series using tight-binding, linear muffin-tin orbital (TB-LMTO) and pseudopotential (VASP) calculations to understand the influences of orbital interactions and valence electron counts on the three observed structural types, as well as to assess reasons for the incommensurately modulated structure of $Eu(Zn_{0.25}Ge_{0.75(2)})_2$, and the general validity of the Zintl−Klemm formalism.

Electronic Structure Calculations

TB-LMTO calculations were carried out in the atomic sphere approximation (ASA) using the Stuttgart program.[9,10] Exchange and correlation were treated by the local spin density approximation.[11] All relativistic effects except spin−orbit coupling were taken into account by using a scalar relativistic approximation.[12] In the ASA method, space is filled with overlapping Wigner-Seitz (WS) spheres. The symmetry of the potential is considered spherical inside each WS sphere, and a combined correction is used to take into account the overlapping part.[13] The radii of WS spheres are obtained by requiring the overlapping potential to be the best possible approximation to the full potential and were determined by an automatic procedure.[13] This overlap should not be too large because the error in kinetic energy introduced by the combined correction is proportional to the fourth power of the relative sphere overlap. No empty spheres were necessary to fill the space of a unit cell. For our calculations on $EuZn_2$, $Eu(Zn_{0.75}Ge_{0.25})_2$, $Eu(Zn_{0.5}Ge_{0.5})_2$, and $Eu(Zn_{0.25}Ge_{0.75})_2$, the WS radii are Eu, 2.241 Å; Zn, 1.351 Å; and Ge, 1.472 Å. For calculations on $EuGe_2$, they are Eu, 2.241 Å and Ge, 1.451 Å. The basis sets included 6s, 6p, and 5d orbitals for Eu; 4s, 4p, and 3d orbitals for Zn; and 4s, 4p, and 4d orbitals for Ge. The Eu 6p and Ge 4d orbitals were treated by the Löwdin downfolding technique,[11,12] and the Eu 4f wave functions were treated as core functions occupied by seven electrons. The crystal orbital Hamilton population (COHP) curves,[14] the integrated COHP values, and electronic densities of states (DOS) were calculated to determine the relative influences of various interatomic orbital interactions. The k-space integrations were performed by the tetrahedron method.[15] Self-consistent charge densities were obtained using a certain number of irreducible k points in the Brillouin zone; these are 280−294 for 10 hexagonal or orthorhombic structural models of $Eu(Zn_{0.5}Ge_{0.5})_2$; 118 for $EuZn_2$, $Eu(Zn_{0.75}Ge_{0.25})_2$, and $Eu(Zn_{0.25}Ge_{0.75})_2$; and 193 for $EuGe_2$. The contribution of the nonspherical part of the charge density to the potential was neglected.

Total energy calculations using the VASP program[16−18] were also conducted for five different models of $Eu(Zn_{0.25}Ge_{0.75})_2$ to identify features of the most energetically favorable layered structure for this Ge-rich composition. This program allows structural relaxations using pseudopotentials and a plane-wave basis set. The Kohn−Sham equations were solved self-consistently using an iterative matrix diagonalization method and an efficient Pulay mixing scheme of the charge density. In this system, we relaxed the z parameter of the Zn/Ge atomic positions simultaneously with the c/a ratio for a set of constant volumes until forces converged to less than 0.005 eV/Å. The ultrasoft Vanderbilt-type pseudopotentials were employed,[19,20] and the valence electrons of the elements included Eu, $5d^16s^2$; Zn, $3d^{10}4s^2$; and Ge, $4s^24p^2$. Convergency was checked with respect to the plane-wave cutoff of 300 eV and the number of k points used in the summation over the Brillouin zone, which were obtained by the Monkhorst−Pack method[21] and sampled on a dense grid of $8 \times 8 \times 8$.

The electron localization function[22] (ELF, η) was evaluated within the TB-LMTO−ASA Stuttgart program package[10] with an ELF module already implemented. To evaluate features of local bonding environments for various compounds, a topological analysis of ELF was conducted with the program *Basin*.[23] The integrated electron density in each basin, which is defined by the surface of zero flux in the ELF gradient, analogous to the procedure proposed by Bader for the electron density,[24] provides the basic information of electron counts for each basin and additionally describes the bonding situation. The software *Amira*[25] was used to visualize ELF distributions of $Eu(Zn_{0.5}Ge_{0.5})_2$ and $EuGe_2$.

Results and Discussion

Electronic structure calculations were conducted on five different compositions of the $Eu(Zn_{1-x}Ge_x)_2$ series based on three different crystal structure types (shown in Figure 1): (1) $EuZn_2$, which adopts the orthorhombic KHg_2-type structure;[26] (2) $Eu(Zn_{0.75}Ge_{0.25})_2$, a hypothetical ternary derivative studied in both the KHg_2-type and AlB_2-type structures; (3) $Eu(Zn_{0.5}Ge_{0.5})_2$, for which 10 different distributions of the Zn and Ge atoms among AlB_2-related models were investigated; (4) $Eu(Zn_{0.25}Ge_{0.75})_2$, based on various planar and puckered 6^3 nets related to AlB_2- and $EuGe_2$-type structures; and (5) $EuGe_2$, which crystallizes in the trigonal $EuGe_2$-type structure.[27]

$EuZn_2$. The 4b-3D net of Zn atoms is constructed by puckered pseudohexagonal 2D layers containing two slightly different Zn−Zn contacts of 2.688 Å and 2.699 Å, layers which are stacked along the c direction to create interlayer Zn−Zn contacts of 2.907 Å. Figure 2 displays its DOS and nearest neighbor Zn−Zn and Eu−Zn COHP curves; the Fermi level (E_F) is shown as a reference energy

(9) Anderson, O. K. *Phys. Rev. B* **1986**, *34*, 2439.
(10) Jepsen, O.; Burkhardt, A.; Andersen, O. K. *The TB-LMTO-ASA Program*, version 4.7; Max-Planck-Institut für Festkörperforschung: Stuttgart, Germany, 1999.
(11) Anderson, O. K.; Jepsen, O. *Phys. Rev. Lett.* **1984**, *53*, 2571.
(12) Andersen, O. K.; Jepsen, O.; Glötzel, D. In *Highlights of Condensed Matter Theory*; Bassani, F., Fumi, F., Tosi, M., Eds.; North-Holland, Lambrecht, W. R. L.: New York, 1985.
(13) Jepsen, O.; Anderson, O. K. *Z. Phys. B* **1995**, *97*, 35.
(14) Dronskowski, R.; Blochl, P. *J. Phys. Chem.* **1993**, *97*, 8617.
(15) Blöchl, P. E.; Jepsen, O.; Anderson, O. K. *Phys. Rev. B* **1994**, *49*, 16223.
(16) Kresse, G.; Hafner, J. *Phys. Rev.* **1993**, *B47*, RC 558.
(17) Kresse, G.; Furthmüller, J. *Phys. Rev.* **1996**, 11169.
(18) Kresse, G.; Furthmüller, J. *Comput. Mater. Sci.* **1996**, *6*, 15.
(19) Vanderbilt, D. *Phys. Rev.* **1990**, *B41*, 7892.
(20) Kresse, G.; Hafner, J. *J. Phys.: Condens. Matter.* **1994**, *6*, 824.
(21) Monkhurst, H. J.; Pack, J. D. *Phys. Rev.* **1973**, *B13*, 518.
(22) (a) Savin, A.; Flad, H. J.; Preuss, H.; von Schnering, H. G. *Angew. Chem.* **1992**, *104*, 185. (b) Savin, A.; Flad, H. J.; Preuss, H.; von Schnering, H. G. *Angew. Chem., Int. Ed. Engl.* **1992**, *31*, 185.
(23) Kohout, M. *BASIN*, version 2.3; Max-Planck-Institut für Chemische Physik fester Stoffe: Dresden, Germany, 2001.
(24) Bader, R. F. W. *Atoms in Molecules: A Quantum Theory*; Oxford University Press: Oxford, U.K., 1999.
(25) *Amira visualization software*; Konrad-Zuse-Zentrum für Informationstechnik Berlin (ZIB): Berlin, Germany, 2003.
(26) Iandelli, A.; Palenzona, A. *Atti Accad. Naz. Lincei Rend. Sci. Fis. Mat. Natur* **1964**, *37*, 165.
(27) Bobev, S.; Bauer, E. D.; Thompson, J. D.; Sarrao, J. L.; Miller, G. J.; Eck, B.; Dronskowski, R. *J. Solid State Chem.* **2004**, *177*, 3545.

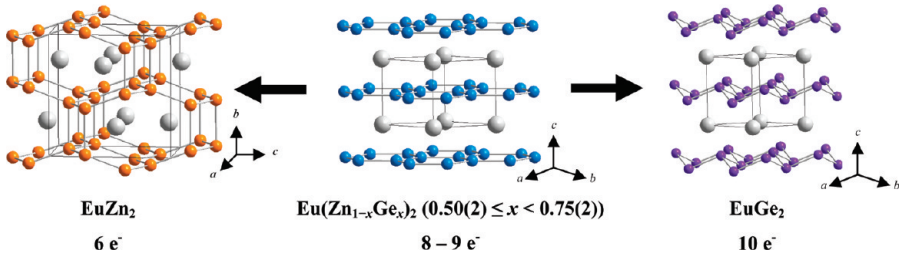

Figure 1. Primary crystal structure types observed for the $Eu(Zn_{1-x}Ge_x)_2$ series: (left) $EuZn_2$ (KHg_2-type; six valence electrons); (middle) $Eu(Zn_{1-x}Ge_x)_2$ ($0.50(2) \leq x < 0.75(2)$, AlB_2-type; eight or nine valence electrons); and (right) $EuGe_2$ ($EuGe_2$-type; 10 valence electrons). Eu, gray; Zn, orange; Zn/Ge, blue; and Ge, purple circles.

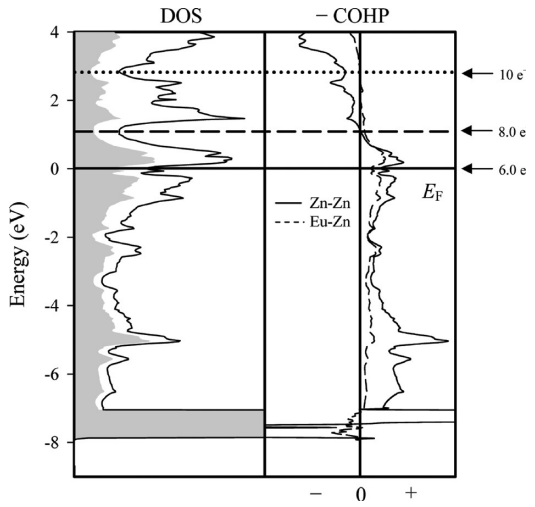

Figure 2. DOS and COHP curves for $EuZn_2$. (Left) Total DOS (solid line), Eu PDOS (white region), and Zn PDOS (gray region). (Right) Eu−Zn and Zn−Zn COHP curves. $E_F(EuZn_2)$ is indicated by the solid line (6.0 e^-) and is the reference. The number of valence electrons that correspond to optima of the Eu−Zn and Zn−Zn COHP curves are also indicated.

value in these curves. E_F falls in a "valley" of the total DOS (TDOS) curve, which lies ca. 1.6 eV below a deeper pseudogap corresponding to 8.0 valence electrons per formula. According to the COHP curves, this pseudogap matches the crossover between Zn−Zn bonding states below and Zn−Zn antibonding states above. Moreover, the Eu−Zn COHP curve reveals significant Eu−Zn bonding between 6.0 and 8.0 valence electrons and then nonbonding character up to ca. 3.0 eV above E_F, that is, ca. 10.0 valence electrons. The TDOS curve up to ca. 2.8 eV below E_F contains more contribution from Zn valence orbitals. However, above this value, Eu 5d and 6s orbitals contribute more than Zn orbitals do to the TDOS. The Zn 3d orbitals are observed in a narrow band, located ca. 7.2−8.0 eV below E_F and, thus, can be treated as formally filled. Empty d-filled d orbital interactions, as seen in Eu 5d−Zn 3d, play an energetic role in stabilizing $EuZn_2$ with respect to alternatives: when Zn 3d orbitals are treated as filled "core" orbitals, their energy is −7.13 eV relative to E_F, whereas when they are included as "valence" orbitals, their band center is −7.49 eV relative to E_F, which provides ca. 3.6 eV of energetic stabilization per Zn atom.

X-ray powder diffraction of Zn-rich $Eu(Zn_{1-x}Ge_x)_2$ phases suggested that Ge atoms could replace small amounts of Zn atoms in the KHg_2-type structure.[1] However, we have no further chemical analysis of these phases and have not identified the upper bound of the single-phase, KHg_2-type $Eu(Zn_{1-x}Ge_x)_2$ region. According to the Zn−Zn and Eu−Zn COHP curves, both interactions show significant bonding overlap above 6.0 valence electrons per formula unit. If a "rigid-band" approximation is assumed, then the calculated electronic structure supports the existence of KHg_2-type, Zn-rich $Eu(Zn_{1-x}Ge_x)_2$ phases. Furthermore, since the unit cell volumes of the supposedly ternary KHg_2-type $Eu(Zn_{1-x}Ge_x)_2$ phases are systematically lower than the volume of $EuZn_2$, it is reasonable to suggest that the additional electrons occupy bonding states in the DOS. Nevertheless, while Zn−Zn and Eu−Zn orbital interactions become enhanced, the DOS value at the revised Fermi level will increase relative to that of $EuZn_2$, which is a frequent signature of an electronic instability.

To check the validity of the "rigid-band" approximation and possible instabilities, we constructed a ternary model of the KHg_2-type structure, $EuZn_{1.5}Ge_{0.5}$, in which the Ge atoms are separated from one another in the 4b-3D net (see Figure 3, left). The complete structural details of this model structure are summarized in the Supporting Information (Table S1). We utilized this separation of Ge atoms on the basis of electronegativity arguments as well as the results of subsequently described calculations of EuZnGe: Ge is the most electronegative element, and there are sufficient numbers of Eu and Zn atoms for Ge atoms to achieve a formal charge of "Ge^{4-}." Moreover, the minimum energy structure of EuZnGe reveals only heteroatomic first- and second-nearest neighbor contacts. The DOSs in addition to Zn−Ge and Zn−Zn COHP curves are illustrated in Figure 3, all of which indicate distinct differences from the DOS and Zn−Zn COHP curves for $EuZn_2$ (Figure 2).

In the DOS, not only does a Ge 4s band appear below −8.0 eV but the Zn 3d band is separated from the valence band but still lies between ca. 7.0 and 8.0 eV below E_F. There remains a pseudogap for 8.0 valence electrons (dashed line), which lies in the midst of Zn−Zn nonbonding states but shows significant Zn−Ge antibonding character. In particular, Zn−Ge orbital interactions are exactly optimized at ca. 6.48 valence electrons, which corresponds to the formulation $Eu(Zn_{0.88}Ge_{0.12})_2$, but become significantly antibonding above ca. 7.26 valence electrons, that is, for $Eu(Zn_{0.69}Ge_{0.31})_2$. The DOS curve in the region of 6.0−6.5(7.3) valence electrons does not show the same increasing DOS values as seen in the curve for $EuZn_2$. Therefore, these results on $EuZn_2$ and a KHg_2-type "$EuZn_{1.5}Ge_{0.5}$" support the existence of a

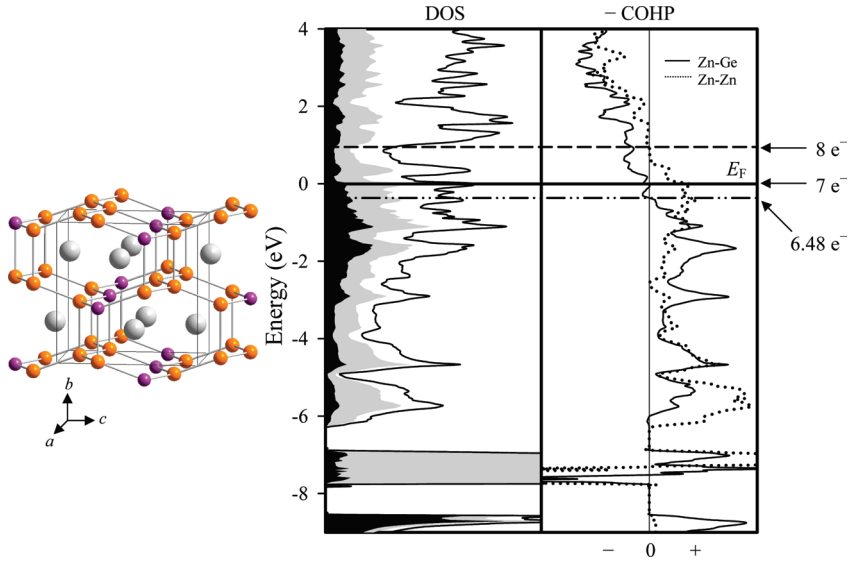

Figure 3. (Left) Crystal structure of KHg_2-type "$Eu(Zn_{0.75}Ge_{0.25})_2$": Eu, gray; Zn, orange; Ge, purple. (Right) Total DOS (solid line), Eu PDOS (white region), Zn PDOS (gray region), and Ge PDOS (black region). Zn−Ge (solid line) and Zn−Zn (dotted line) COHP curves. E_F (solid line) is the energetic reference (0 eV).

homogeneity width for the KHg_2-type structure in the Zn-rich region of $Eu(Zn_{1-x}Ge_x)_2$ phases, with the maximum Ge content lying between ca. 12 and 30 atom %.

AlB_2-Type $Eu(Zn_{0.75}Ge_{0.25})_2$. Experimental evidence indicates that the AlB_2-type structure emerges in the $Eu(Zn_{1-x}Ge_x)_2$ system when x exceeds 0.50(2), that is, at EuZnGe. As mentioned above, for reactant mixtures that were Zn-rich, that is, $x < 0.50$, KHg_2-type phases were observed, but so was an AlB_2-type phase with constant composition, $Eu(Zn_{0.50}Ge_{0.50(2)})_2$, as evaluated by energy-dispersive X-ray spectroscopy and X-ray powder diffraction.[1] Therefore, to investigate the phase segregation of Zn-rich, AlB_2-type $Eu(Zn_{1-x}Ge_x)_2$ phases, we constructed a hypothetical Zn-rich compound, $Eu(Zn_{0.75}Ge_{0.25})_2$, with planar 6^3 nets, shown in Figure 4 (left). As described in the previous subsection, first- and second-nearest neighbor Ge−Ge contacts were eliminated in this model, which, therefore, required an orthorhombic cell (ca. $2a_{hex} \times 2\sqrt{3}a_{hex} \times 2c_{hex}$), space group *Fmmm*, and two 6^3 nets per cell (see structural details in Supporting Information, Table S1). The DOS and nearest neighbor Zn−Zn and Zn−Ge COHP curves for this model are shown in Figure 4 (right), results which show similarities as well as significant differences from analogous curves calculated for the KHg_2-type model, $Eu(Zn_{0.75}Ge_{0.25})_2$, shown in Figure 3. In both cases, the Zn 3d orbitals are located around 7 eV below E_F, but the bandwidth is ca. 20% larger in the AlB_2-case, which is due primarily to the shorter Zn−Ge distances in the 6^3 nets and larger Zn−Ge orbital overlaps. Moreover, a narrow, primarily Ge 4s band occurs ca. 9 eV below E_F. The valence band is dominated by Zn 4s states between ca. −6 and −4 eV and then switches to mostly Ge 4p states. Unlike the KHg_2 case, there is no pseudogap in the TDOS curve for the AlB_2-type model, $Eu(Zn_{0.75}Ge_{0.25})_2$, near 8.0 valence electrons. Rather, a modest minimum occurs at 9.5 valence electrons (ca. +1.8 eV), and a deep pseudogap occurs at 10.0 valence electrons. The Zn−Ge COHP curve shows nonbonding character between ca. 7.0 and 9.5 valence electrons, before developing

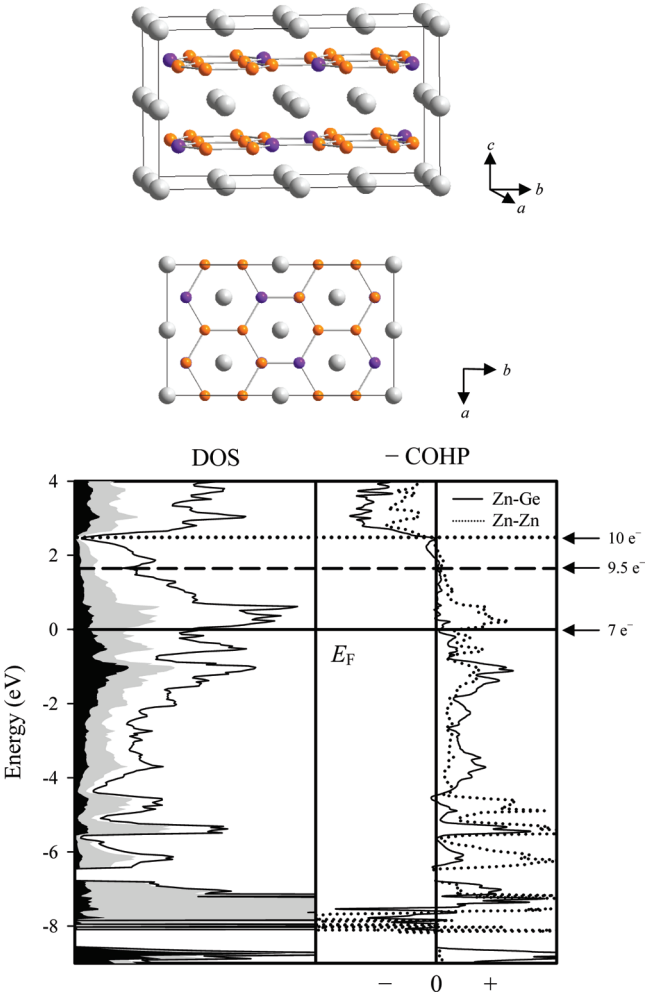

Figure 4. Structure and DOS and COHP curves for AlB_2-derived $Eu(Zn_{0.75}Ge_{0.25})_2$. (Top) Structure projected along *a* and *c* directions. (Bottom) Total DOS (solid line), Eu PDOS (white region), Zn PDOS (gray region), and Ge PDOS (black region) as well as Zn−Ge (solid line) and Zn−Zn (dotted line) COHP curves. E_F (solid line) is the energetic reference (0 eV). The numbers of valence electrons for two minima in the TDOS curve are also shown.

antibonding character. On the other hand, the Zn−Zn COHP curve shows strong bonding character at and above E_F for 7.0 electrons and achieves optimization at ca. +2.5 eV for 10.0 electrons. This crossover corresponds to 10 valence electrons, and a deep pseudogap is observed in a TDOS curve. In fact, although the Zn−Zn COHP curve is similar to that of $EuZn_2$, the Zn−Zn COHP curve is quite different. The total electronic energy of this AlB_2-type Zn-rich compound was calculated and compared against the mean total electronic energy of KHg_2-type $EuZn_2$ and AlB_2-type $Eu(Zn_{0.5}Ge_{0.5})_2$. For this energetic comparison, the radii of the WS spheres of each element were set equal to minimize computational differences. The computational result indicated that the two distinct phases, $EuZn_2$ and $Eu(Zn_{0.5}Ge_{0.5})_2$, are more favorable by 116.6 meV than the single AlB_2-type $Eu(Zn_{0.75}Ge_{0.25})_2$, which agrees with experimental results.[1] Although it is inherently difficult to revoke the existence of a chemical structure and composition, there are no features in its electronic structure, either DOS or COHP curves, to identify specific stability criteria.

AlB_2-Type $Eu(Zn_{0.5}Ge_{0.5})_2$. Due to the small difference between the X-ray scattering factors of Zn and Ge, no indication of long-range ordering of these two elements could be detected by X-ray diffraction experiments within or perpendicular to the 6^3 nets. However, a certain degree of short-range ordering can be considered between Zn and Ge atoms.[28,29] Thus, we constructed 10 ternary structural models (see Figure 5) to account for the different nearest and second-nearest neighbor contacts among the Zn and Ge atoms. To create these models of $Eu(Zn_{0.5}Ge_{0.5})_2$, both hexagonal and orthorhombic unit cells are needed. The orthorhombic unit cell is obtained by transforming the hexagonal AlB_2-type structure into an orthorhombic setting via a *translationengleiche* transformation[30] of index 3 (*t*3) and followed by subsequent adjustments along the stacking direction of the 6^3 nets depending upon the corresponding atomic arrangements. Detailed structural information of these models is listed in the Supporting Information (Table S2).

Models 1−3 contain alternating Zn and Ge atoms on the 6^3 sheets, where each Zn/Ge atom is connected to three Ge/Zn atoms. They differ from each other in how the 6^3 sheets stack along the *c* axis: (1) eclipsed to create just Zn···Zn and Ge···Ge interactions between planes, space group $P6m\bar{2}$, $Z = 1$; (2) alternating to create only Zn···Ge interactions between planes, space group $P6_3/mmc$, $Z = 2$; and (3) a 1:1 intergrowth of models 1 and 2 to create Zn···Ge, Zn···Zn, and Ge···Ge interactions between planes, space group $P6_3/mmc$, $Z = 4$. On the other hand, homoatomic Zn−Zn and Ge−Ge contacts occur within the 6^3 nets for models 4−10. In models 4−6, Zn and Ge atoms alternate along one axis, forming heteroatomic zigzag chains, whereas homoatomic Zn−Zn or Ge−Ge bonds exist along the orthogonal axis. Three different stacking sequences of these 6^3 nets are the same as those of models 1−3, and the unit cells are orthorhombic. For models 7−9, Zn/Ge atoms form homoatomic zigzag chains along one axis, whereas heteroatomic Zn−Ge bonds exist along the orthogonal axis. Again, three different stacking sequences are created; all unit cells are orthorhombic. Finally, model 10 is hexagonal, consisting of Zn-only and Ge-only 6^3 nets alternating along the *c* axis.

On the basis of the numbers of the heteroatomic and homoatomic interactions in the 6^3 nets, these 10 models of EuZnGe can be categorized into four groups: (A) models 1−3, three heteroatomic interactions; (B) models 4−6, two hetero- and one homoatomic interaction; (C) models 7−9, one hetero- and two homoatomic interactions; and (D) model 10, three homoatomic interactions. As the 6^3 net contains more heteroatomic Zn−Ge interactions, the structure is energetically more favorable. Therefore, models 2 and 3 of group A are more stable than all models in group B. In the same sense, all models in group B are more stable than the models in group C. Although model 1 in group 1 is exceptional from this trend, model 10 is indisputably the least stable. Among models in each group, interlayer atomic interactions also play an important role, which affects structural stability. However, because of the relatively longer interlayer atomic distances and intervention of Eu 5d orbitals located between these layers, the number of heteroatomic interactions among models in the same group is not significantly as decisive as among different groups to reveal the energetically most stable structure. According to total electronic energies included in Figure 6, model 2 is energetically the most favorable structure, which contains only heteroatomic Zn−Ge interactions within and perpendicular to the hexagonal nets. Thus, although we cannot observe atomic ordering between Zn and Ge using X-ray diffraction, short-range in-plane and out-of-plane ordering should be considered. Therefore, all subsequent theoretical calculations for $Eu(Zn_{0.5}Ge_{0.5})_2$ are conducted using model 2. Figure 6 displays DOS and COHP curves of this equiatomic compound, where E_F is the reference energy value and is located slightly above a pseudogap in the DOS. These DOS and COHP curves are very similar to those of EuGaSi, which also adopts a ternary version of the AlB_2-type structure.[8] Throughout the entire DOS curve, significant mixing between valence orbitals of Eu, Zn, and Ge atoms is observed. The region below E_F shows significant contributions from Ge 4p and Eu 5d orbitals with small contributions from Zn 4s and 4p, whereas the region above E_F is dominated by Eu 5d orbitals.

The DOS curves, as well as the electronic band structures (available in Supporting Information, Figures S1 and S2), indicate that the majority of Ge 4p orbitals are located mostly within 5 eV below E_F, implying that they are formally filled with electrons, whereas the majority of Zn 4s and 4p orbitals are centered far above E_F, between 7 and 15 eV above E_F, suggesting that they are formally empty. Furthermore, E_F for EuZnGe falls in a deep pseudogap of the TDOS curve. Our experimental results revealed a Zn−Ge bond distance of 2.5190(3) Å on the hexagonal nets,[1] which is significantly shorter than the sum of 12-coordinate metallic radii of Zn and Ge (2.772 Å: r(Zn) = 1.394 Å, r(Ge) = 1.378 Å[31]), but are in

(28) Pöttgen, R. *Z. Kristallogr*. **1995**, *210*, 924.
(29) Buschow, K. H. J.; Schobinger-Paramatellos, P.; Fischer, P. *J. Less-Common Met*. **1988**, *39*, 221.
(30) Bärnighausen, H. *MATCH* **1980**, *9*, 139.
(31) Teatum, E.; Gshneidner, K., Jr.; Waber, J. *Radii of the Elements for CN12*; U. S. Department of Commerce: Washington, DC, 1960; LA-2345.

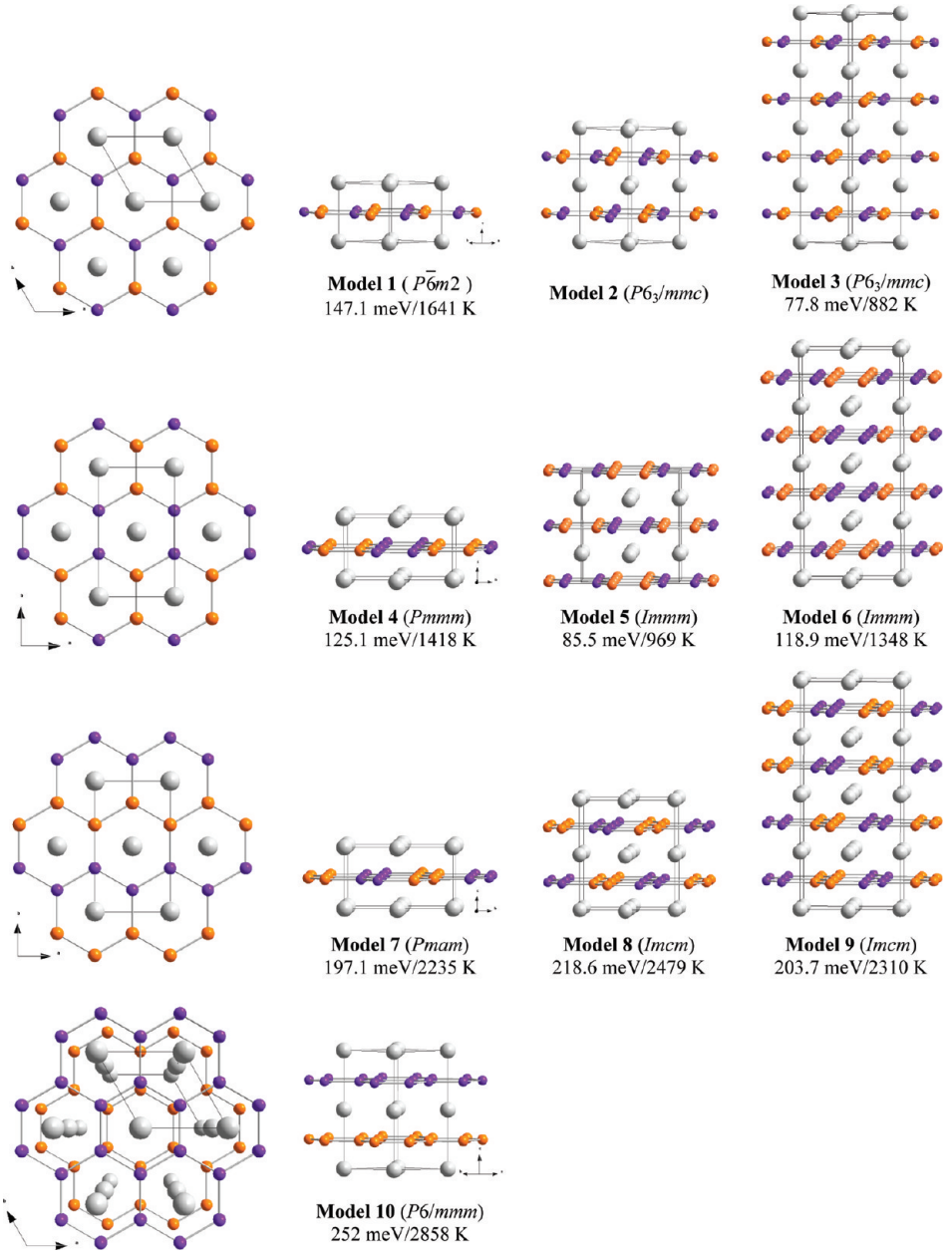

Figure 5. Ten structural models of $Eu(Zn_{0.5}Ge_{0.5})_2$. See text for detailed descriptions: Eu, gray; Zn, orange; Ge, purple circles. The relative total electronic energies per formula unit are listed as compared to model 2; space groups can adopt nonstandard settings.

excellent agreement with the sum of their covalent radii (2.47 Å: r(Zn) = 1.25 Å, r(Ge) = 1.22 Å[32]). Moreover, the average Zn−Zn and Ge−Ge distances in $EuZn_2$ (2.699 Å)[26] and $EuGe_2$ (2.564(4) Å)[27] fall between the corresponding sums of metallic and covalent radii. Therefore, the observed Zn−Ge bond distances indicate strong polar covalent interactions within the polyanionic nets. According to the fatband analyses of the band structure, shown in the Supporting Information (Figures S1 and S2), this Zn−Ge distance can be attributed to participation of both σ-bonding interactions, which correspond to the bands spanning between ca. 6 and 0.2 eV below E_F, and π-bonding interactions, which correspond to bands starting ca. 4.2 eV below E_F. The importance of these Zn−Ge π interactions is reinforced when compared to the computational results on a 4b-3D "EuZnGe" in the hexagonal LiGaGe-type structure:[33] with respect to model 2, this 4b-3D hypothetical structure is ca. 1.00 eV per formula unit higher in energy, although Zn−Ge orbital interactions are optimized, and the Fermi level lies in a pseudogap in the DOS curve (see the Supporting Information, Table S3 and Figure S3).

Therefore, the 6^3[ZnGe] net behaves like eight-electron graphite layers, and its chemical bonding can be understood using the Zintl−Klemm concept.[2−4] Magnetic susceptibilities further validate divalent Eu, so EuZnGe can be formulated as $Eu^{2+}[ZnGe]^{2-}$.[1] Interactions between [ZnGe] planes occur along the c axis via Eu 5d orbitals, some of which drop below E_F (see Figures S1

(32) Emsley, J. *The Elements*; Clarendon Press: Oxford, U. K., 1998.

(33) Bockelmann, W.; Jacobs, H.; Schuster, H. U. *Z. Anorg. Allg. Chem.* **1974**, *410*, 233.

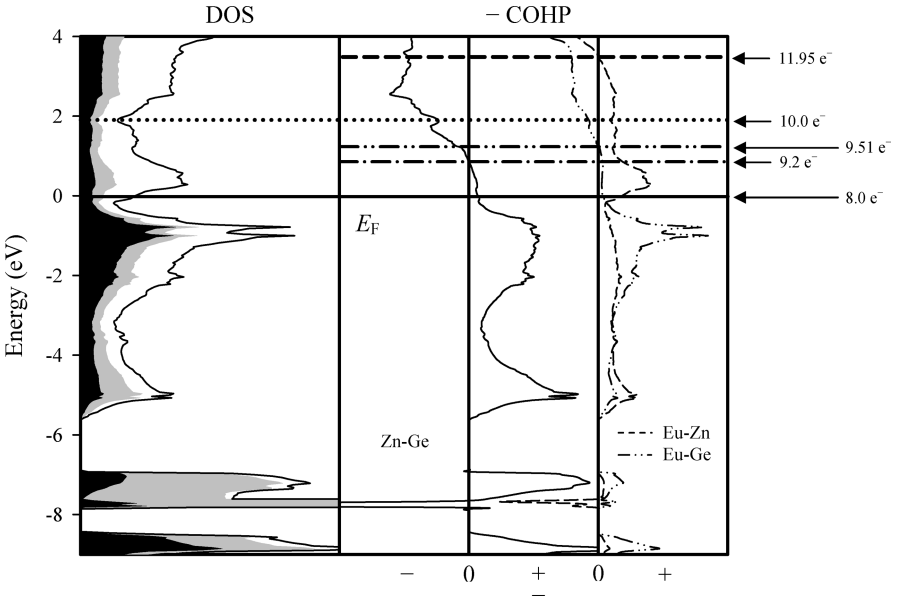

Figure 6. DOS and COHP curves for $Eu(Zn_{0.5}Ge_{0.5})_2$. (Left) Total DOS (solid line), Eu PDOS (white region), Zn PDOS (gray region), and Ge PDOS (black region). (Right) Zn−Ge, Eu−Zn and Eu−Ge COHP curves. E_F (solid line) is the energetic reference (0 eV). The numbers of valence electrons, which correspond to local minima in the TDOS curve as well as optima of the COHP curves are also shown.

and S2, Supporting Information). Thus, Zn−Ge orbital interactions are predominantly two-dimensional in character.[8,34]

In the Zn−Ge COHP curve (Figure 6, right), bonding character changes to antibonding character at ca. 1.2 eV above E_F, which corresponds to 9.2 valence electrons. As discussed earlier for Zn−Zn contacts in the 4b-3D nets of $EuZn_2$, this COHP result implies that these Zn/Ge 6^3 nets can accept additional valence electrons. Moreover, Eu−Ge and Eu−Zn COHP curves also show bonding or nonbonding character up to this energy value. Therefore, the ternary AlB_2-type structure in the Eu−Zn−Ge system can accommodate more than 8.0 valence electrons and can adopt Ge-rich compositions without building up antibonding character within the nearest neighbor contacts, which is responsible for the decreasing *a* axis in the observed AlB_2-type $EuZn_{1-y}Ge_{1+y}$ phases as well as being eventually influential to the phase separation into the AlB_2-type and the $EuGe_2$-type structures. Although Eu−Ge and Eu−Zn COHP curves maintain their bonding character, respectively, up to 9.51 and 11.95 valence electrons, we do not expect more than approximately 9.2 valence electrons for the upper bound of the AlB_2-type phase because the Zn−Ge COHP develops significant antibonding character beyond ca. 1.2 eV above E_F. Therefore, on the basis of COHP analyses, we expect that the experimentally obtainable upper bound of the AlB_2-type phase can be approximately $Eu(Zn_{0.20}Ge_{0.80})_2$. According to our experiments, this upper bound composition is $Eu(Zn_{0.30(2)}Ge_{0.70(2)})_2$ containing 8.8 valence electrons.[1] This poor agreement with the observed upper bound may be due to the limitation of the "rigid-band" approximation applied in this analysis, which was already apparent for the Zn-rich phases. Therefore, we investigated a specific Ge-rich model, $Eu(Zn_{0.25}Ge_{0.75})_2$.

AlB_2-Type $Eu(Zn_{0.25}Ge_{0.75})_2$. The structural model created for the nine-electron $Eu(Zn_{0.25}Ge_{0.75})_2$ resembles that for $Eu(Zn_{0.75}Ge_{0.25})_2$ shown previously, but with a larger unit cell volume and switched Zn and Ge positions (see the Supporting Information, Table S4). In this model (see Figure 7), the minority Zn atoms are isolated from one another throughout the structure, which minimizes the numbers of homoatomic interactions. Figure 7 illustrates DOS and nearest neighbor COHP curves for this model. Given the Ge-rich composition, the Ge PDOS is more pronounced than the Zn PDOS throughout the entire DOS curve. A pseudogap, which was clearly observed just below E_F in the DOS diagram of $Eu(Zn_{0.5}Ge_{0.5})_2$ (Figure 6) is no longer noticeable because of the more pronounced contribution from Eu 5d and Ge 4p orbitals near E_F. The Zn−Ge COHP curve is fully optimized at E_F, while the Ge−Ge COHP curve falls well into a strong antibonding region. The Ge−Ge COHP curve is optimized at ca. 7.63 electrons. Thus, the change in composition from EuZnGe to $Eu(Zn_{0.25}Ge_{0.75})_2$ significantly affects the calculated DOS and predicts a lower upper bound for the AlB_2-type structures than suggested by analysis of the DOS and COHP curves for EuZnGe. According to the COHP analysis of $Eu(Zn_{0.25}Ge_{0.75})_2$, moreover, planar 6^3 nets are not especially favorable environments to accommodate the Ge−Ge orbital interactions. Thus, the crystal structure may undergo some type of structural or electronic distortion, or even phase separation to remove this instability. In fact, during the structure refinements of the AlB_2-type $EuZn_{1-y}Ge_{1+y}$ phase,[1] we observe a distinct increase of U_{33}/U_{11} ratios at the 2d (Zn/Ge) sites as the Ge content increases, an observation which indicates an increasing tendency toward puckering of the 6^3 nets.[8,35] Although this ratio is 1.9 in $Eu(Zn_{0.5}Ge_{0.5})_2$ and increases to 7.0 in $Eu(Zn_{0.30(2)}Ge_{0.70})_2$, all refinement attempts converge toward

(34) Pöttgen, R. *J. Alloys. Comp.* **1996**, *243*, L1.

(35) You, T.-S.; Zhao, J.-T.; Pöttgen, R.; Schnelle, W.; Burkhardt, U.; Grin, Y.; Miller, G. J. *Chem. Mater.* **2009**, Submitted for publication.

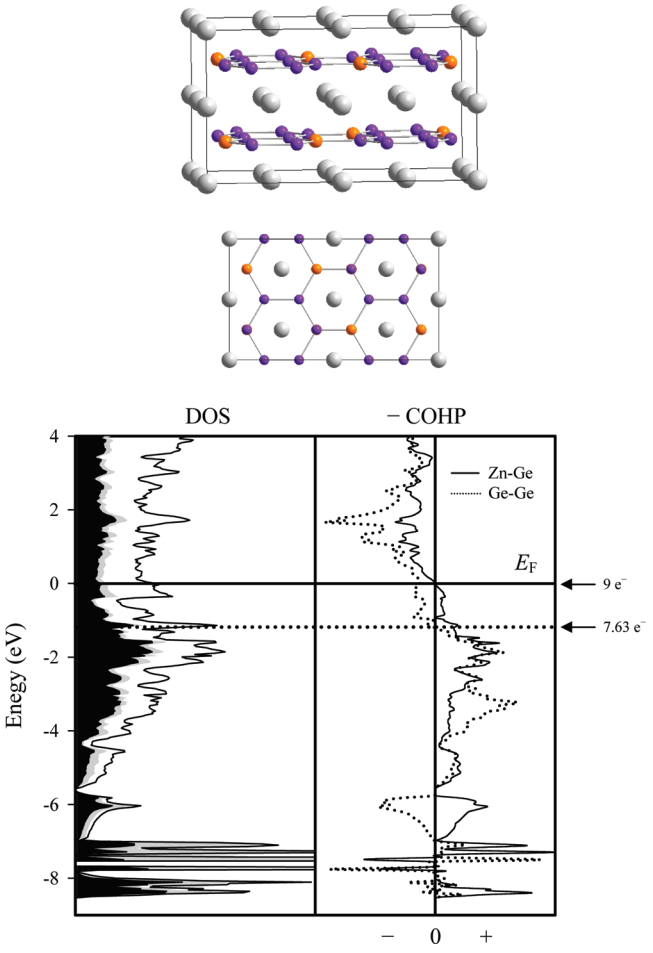

Figure 7. Structure and DOS and COHP curves for AlB_2-derived Eu$(Zn_{0.25}Ge_{0.75})_2$. (Top) Structure projected along *a* and *c* directions. (Bottom) Total DOS (solid line), Eu PDOS (white region), Zn PDOS (gray region), and Ge PDOS (black region) as well as Zn−Ge (solid line) and Ge−Ge (dotted line) COHP curves. E_F (solid line) is the energetic reference (0 eV). The numbers of valence electrons for two optima in the COHP curves are also shown.

planar 6^3 nets, even when space groups are selected that allow the *z* parameter of the 2d (Zn/Ge) sites to be unrestricted. However, in Eu$(Zn_{0.25(2)}Ge_{0.75(2)})_2$, an incommensurately modulated structure along the *c* direction was observed, and its solution relied on a 3 + 1 D super space analysis with twinning. The resulting structural model shows puckering of the 6^3 nets, which is rather constant and changes direction at regular intervals along the stacking direction. Presumably, further details of the model are influenced by how Zn and Ge are distributed throughout the entire arrangement, but this effect could not be solved by X-ray diffraction results. More details of this structure can be found in our companion article.[1]

To investigate puckered versus planar hexagonal layers for Eu$(Zn_{0.25}Ge_{0.75})_2$, we performed a series of total energy and structural relaxation calculations using the VASP code[16−18] for five different, initial hypothetical models (Figure 8) of Eu$(Zn_{0.25}Ge_{0.75})_2$. In models 1−4, each hexagonal layer has a fixed composition $[Zn_{0.5}Ge_{1.5}]$ with identical lattice parameters and the Zn atoms separated completely from one another. These layers are planar in model 1, while models 2−4 contain puckered sheets. Model 2 contains in-phase puckered layers along the *c* axis, whereas model 3 has out-of-phase puckered layers, which form closer interlayer Zn···Ge and Ge···Ge interactions. Model 4 includes different types of out-of-phase puckered layers from model 3, in which all Ge sites have pyramidal local environments (as in model 3), whereas all Zn sites maintain locally planar environments (as in model 1). In model 5, planar equiatomic [ZnGe] hexagonal layers alternate with puckered Ge-only layers, that is, a 1:1 intergrowth structure of EuZnGe and $EuGe_2$. Further details of these structural models are summarized in the Supporting Information (Table S3).

Upon structural relaxation, all models displayed changes from their initial configurations (see also Figure 8). In general, the initially puckered 6^3 nets in models 2−4 became less puckered. The puckered $[Ge_2]$ nets in model 5 became exactly planar, and the planar nets in model 1 remained planar but moved further apart, that is, increased the *c*-axis length. The relative total energies of the initial and relaxed models are also compared in Figure 8. All relaxed models exhibit lower energies than their initial models. In particular, model 3a with out-of-phase puckered layers is the most favorable structure, but model 2a with in-phase puckered layers is just 5.2 meV/fu higher in energy than model 3a. In models 3a and 2a, the angular deficiencies of the sum of the three bond angles from 360° at each atomic site, which is a measure of pyramidalization, are 16.2° for the Zn site and 15.4° and 17.7° for the Ge sites. These values compare very favorably with the range 8.2−18.4° calculated from the incommensurately modulated solution.[1] In addition, we also observed a ca. 10% increase of the *c*/*a* ratio in model 3a after structure relaxation from model 3, which suggests net repulsive interactions between the 6^3 nets. The energetic similarity between models 2a and 3a substantiate the super space solution for this incommensurately modulated structure. Puckering of each 6^3 net is intrinsic with the Zn and Ge atoms uniformly distributed throughout each network. The significantly higher energies of models 5 and 5a, together with relaxation toward planar [ZnGe] and $[Ge_2]$ nets, discounts this type of intergrowth as a reasonable solution to the structure of Eu$(Zn_{0.25}Ge_{0.75(2)})_2$.[1]

The effect of puckering on the DOS as well as Zn−Ge and Ge−Ge COHP curves is presented in Figure 9, which shows these curves based on a TB-LMTO−ASA calculation of model 2a obtained by VASP, and should be compared against Figure 7. At nine valence electrons, Zn−Ge orbital interactions are optimized, but there are two significant differences between the two figures that favor the puckered model: (i) E_F falls in a narrow pseudogap of the DOS of the puckered model as compared to the planar case, and (ii) the Ge−Ge COHP curve is essentially nonbonding in the puckered case, where it is distinctly antibonding in the planar case. Both of these features in the electronic structure contribute to the preference toward puckering of the 6^3 nets in Eu$(Zn_{0.25}Ge_{0.75(2)})_2$.

Bonding Analysis by the Electron Localization Function. The elements of chemical bonding are consequently derived by employing the topological features of a bonding-detector function, for example, the ELF,[22] which is related to the motion of electron pairs in a chemical system. The directed interaction between atoms in a

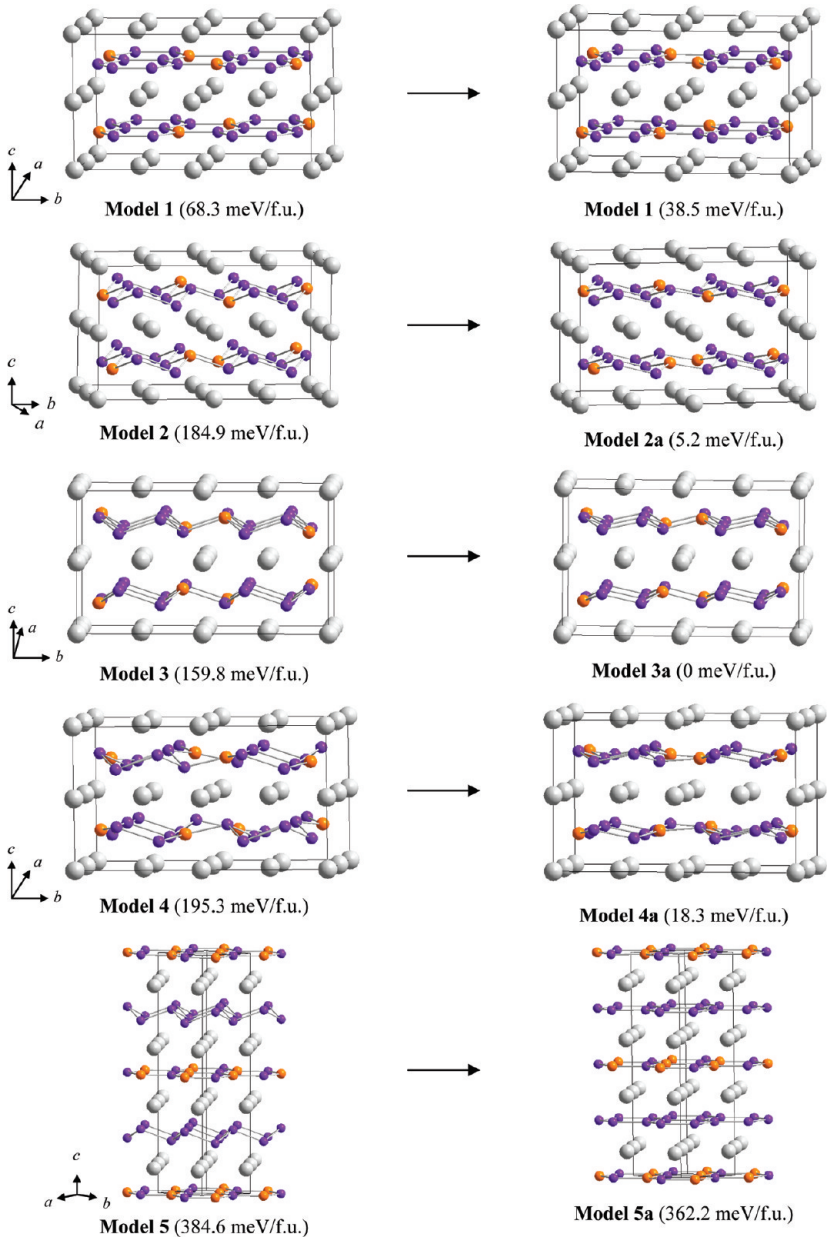

Figure 8. Five structural models of $Eu(Zn_{0.25}Ge_{0.75})_2$ before (left column) and after (right column) relaxation. Total energies relative to model 3a are noted.

chemical structure can be distinguished in real space. Maxima of the ELF in the valence region (valence shells)[36] provide signatures for directed (covalent) bonding. This analysis of the topology of ELF can be combined with the consecutive integration of the electron density in "basins," which are bound by zero-flux surfaces in the ELF gradient field.[23] This procedure, similar to the one proposed for electron density,[24] allows assignment of an electron count for each basin, revealing basic information about chemical bonding.

The ELF can be illustrated in two distinct ways: (1) as surfaces corresponding to a single ELF value ("isosurfaces") and (2) as a slice through the structure. To achieve further insights into the valence region of $Eu(Zn_{0.5}Ge_{0.5})_2$, especially whether there exists any interlayer interaction between 6^3 sheets, for example, two-center, two-electron bonds between interlayer Zn···Ge contact or multicentered interactions involving Zn/Ge and Eu atoms, as observed in EuGaSn,[8] ELF was analyzed carefully. To have reference systems for comparison, the ELF analyses on $EuZn_2$ and $EuGe_2$ were also completed. The ELF contributions of $Eu(Zn_{0.5}Ge_{0.5})_2$ and $EuGe_2$ are illustrated using both "isosurfaces" and a slice, whereas that of $EuZn_2$ is displayed using slices of different planes.

$EuZn_2$. ELF analysis indicates that four bond attractors, which are defined as local maxima of the ELF values, exist around each Zn atom. As shown in Figure 10, each Zn atom forming 4b-3D nets with locally distorted tetrahedral coordination is connected to two other Zn atoms, respectively, along the *b* direction, creating 2D chains with distances of 2.688−2.907 Å, and along the *a* direction, forming 2D zigzag chains with a bond distance

(36) Kohout, M.; Wagner, F. R.; Grin, Yu. *Theor. Chem. Acc.* **2002**, *108*, 150.

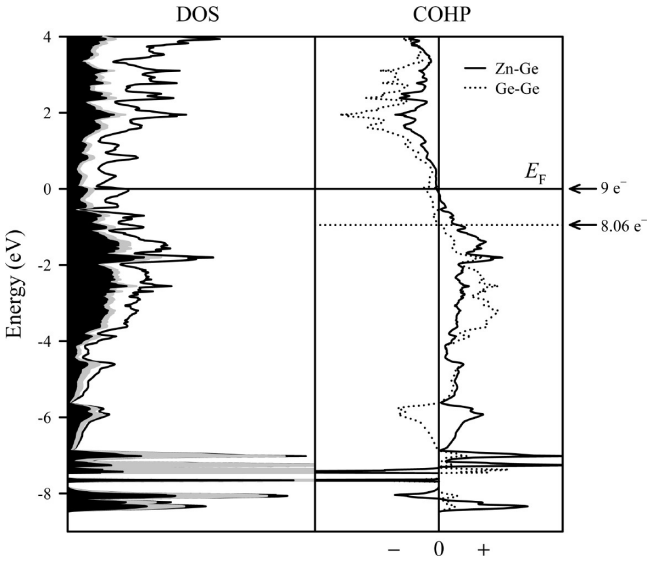

Figure 9. Structure and DOS and COHP curves for minimum energy structure of $Eu(Zn_{0.25}Ge_{0.75})_2$ as determined by VASP (model 3a). Total DOS (solid line), Eu PDOS (white region), Zn PDOS (gray region), and Ge PDOS (black region) as well as Zn−Ge (solid line) and Ge−Ge (dotted line) COHP curves. E_F (solid line) is the energetic reference (0 eV). The numbers of valence electrons for two optima in the COHP curves are also shown.

of 2.699 Å. Since there exist only Zn−Zn homoatomic bonds, bond attractors are observed in the midst of two neighboring Zn atoms.

$Eu(Zn_{0.5}Ge_{0.5})_2$. Two types of ELF attractors are located around the 3b-2D Zn and Ge atoms showing trigonal-planar coordination in the 6^3 sheets. In Figure 10, lone-pair-like attractors are detected symmetrically above and below Ge atoms along [001] together with bond attractors on Zn−Ge bonds in the 6^3 sheets. Because of the different electronegativities of Zn and Ge (Pauling scale, χ (Zn) = 1.65 and χ (Ge) = 2.01),[32] electrons are more localized around Ge than around Zn. This electron localization is significantly more pronounced than those observed for Ga−Si bonds in EuGaSi or for Ga−Sn bonds in EuGaSn.[8] However, no attractor is detected between interlayer Zn···Ge contacts. This implies that the alternating stacking patterns of the 6^3 sheets along the *c* axis are not caused by an attractive interaction between Zn···Ge contacts but rather are caused by a repulsive interaction between interlayer Ge atoms surrounded by electron pairs. Integration of the total electron density within each basin gives values of 2.31 electrons for the valence shell basins of Zn and 5.84 electrons for the valence shell basins of Ge, for a formulation of $Eu^{2.15+}[Zn^{0.31-}Ge^{1.84-}]$ with roughly divalent Eu atoms.

$EuGe_2$. The topological analysis of ELF reveals four attractors around each Ge atom creating 3b-2D puckered hexagonal nets with local trigonal-pyramidal environments, as shown in Figure 10. One lone-pair-like attractor is located above (or below) Ge atoms along [001], and three other attractors are symmetrically located in the midst of Ge−Ge contacts. Integration of the total electron density within each basin gives valence electron counts of 2.49 electrons for the lone-pair-like attractor and 1.76 electrons for the Ge−Ge bond attractors. Thus, the total valence electron count for valence shell basin sets is

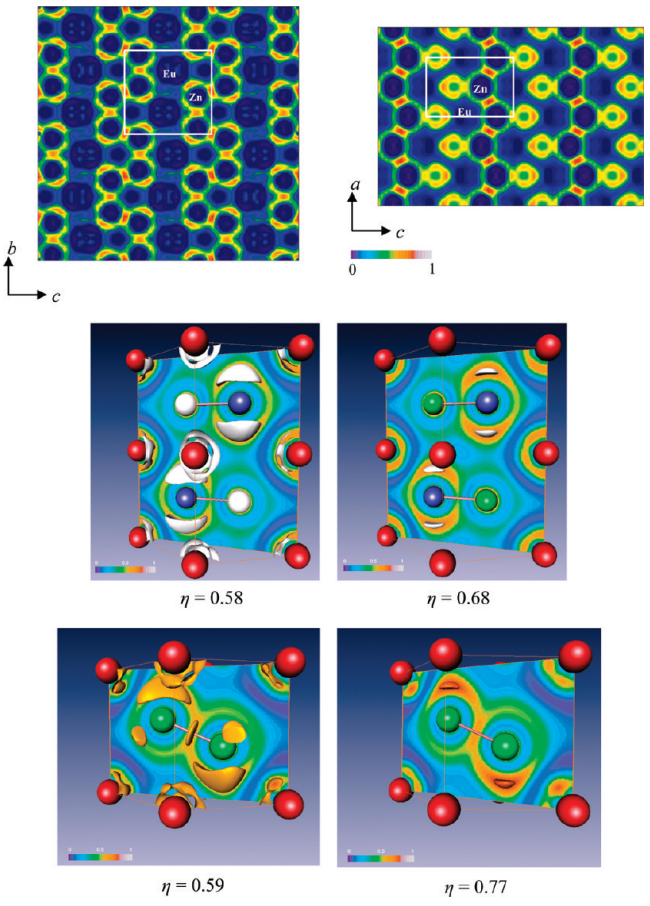

Figure 10. (Top) ELF distributions, depicted as filled contour slices, for $EuZn_2$. Left: (1 0 0) slice, a = 0. Right: (0 1 0) slice, b = 0.06. (Middle) ELF distributions in $Eu(Zn_{0.5}Ge_{0.5})_2$: Eu sites, red spheres; Zn sites, green spheres; Ge sites, blue spheres. ELF isosurfaces (η = 0.58 and 0.68), colored in white, produce attractors associated with Zn and Ge atoms. A (110) ELF slice is also illustrated. (Bottom) ELF distributions in $EuGe_2$: Eu sites, red spheres; Ge sites, green spheres. ELF isosurfaces (η = 0.59 and 0.77), colored in yellow, produce attractors associated with Ge lone pairs and a Ge−Ge bond. A (110) ELF slice is also illustrated.

5.13 electrons per Ge atom (= 2.49 e^- ("lone pair") + 3 × 1.76 $e^-/2$ ("bond pairs")), which can be written as $Ge^{1.13-}$. As a result, the bonding situation in $EuGe_2$ can be described as $Eu^{2.26+}[Ge^{1.13-}]_2$, which agrees reasonably well with a Zintl−Klemm representation as $Eu^{2+}[Ge^-]_2$.

Summary

We have conducted a series of electronic structure calculations for the observed and hypothetical structural models of the $Eu(Zn_{1-x}Ge_x)_2$ ($0 \le x \le 1$) system using both TB-LMTO−ASA and VASP methods. The experimentally observed homogeneity width of the $EuZn_2$ phase can be understood from the Zn−Zn COHP curve showing significant bonding character at E_F. The DOS and COHP analyses for the hypothetical Zn-rich compound prove that the compound should prefer to exist as two distinct phases rather than to keep a Zn-rich composition in the AlB_2-type structure. Total electronic energy comparison for 10 possible equiatomic models indicates that the more heteroatomic interactions that exist in a unit cell, the more energetically favorable a structure it is. DOS curves and band structures show that the observed bond distance between Zn and Ge on the hexagonal nets can be attributed to both σ- and π-bond

interactions. The observed homogeneity width of the AlB_2-type structure can be explained using COHP analysis of Eu$(Zn_{0.5}Ge_{0.5})_2$. The calculations on the Ge-rich model revealed that Zn−Ge bonding is energetically favored, whereas Ge−Ge bonding is unfavored on the planar 6^3 net environment in the AlB_2-type structure. VASP results from structure relaxation are consistent with the observed incommensurately modulated super structure. ELF analysis for the equiatomic compound indicates that the alternating stacking patterns of 6^3 sheets along the *c* axis are not caused by an attractive interaction between Zn···Ge contacts but rather are caused by repulsive interaction between interlayer Ge atoms containing localized electrons around them.

Acknowledgment. This work was supported by NSF DMR 02-41092 and 06-05949.

Supporting Information Available: Structural information for various models of Eu$(Zn_{0.75}Ge_{0.25})_2$, Eu$(Zn_{0.5}Ge_{0.5})_2$, and Eu$(Zn_{0.25}Ge_{0.75})_2$ studied by TB-LMTO-ASA and VASP calculations and electronic band structures for Eu$(Zn_{0.5}Ge_{0.5})_2$ (model 2). This material is available free of charge via the Internet at http://pubs.acs.org.